Comments on Inorganic Chemistry
Publication details, including instructions for authors and subscription information:
http://www.informaworld.com/smpp/title~content=t713455155

The Use of Non-Covalent Interactions in the Assembly of Metal/Organic Supramolecular Arrays

A. S. Borovik[a]
[a] Department of Chemistry, University of Kansas, Lawrence, KS

Online publication date: 14 September 2010

To cite this Article Borovik, A. S.(2002) 'The Use of Non-Covalent Interactions in the Assembly of Metal/Organic Supramolecular Arrays', Comments on Inorganic Chemistry, 23: 1, 45 — 78
To link to this Article: DOI: 10.1080/02603590214376
URL: http://dx.doi.org/10.1080/02603590214376

The Use of Non-Covalent Interactions in the Assembly of Metal/Organic Supramolecular Arrays

A.S. BOROVIK*

Department of Chemistry,
University of Kansas, Lawrence, KS 66045

(Received March 05, 2001)

The design and synthesis of molecules that can organize into specific supramolecular assemblies in the solid state is an area of considerable interest, since incorporation of specific structural components into a crystal lattice may lead to new materials with desirable chemical and physical properties. However, it is still difficult to reliably predict crystal structures especially those in non-centrosymmetric space groups. To develop compounds whose assembly is more controlled and predictable, we are investigating the formation of supramolecular assemblies from C_2- and C_3-symmetric molecular species. The C_2-symmetric systems use a rigid template to control the orientation of appended groups. Using hydrogen bonds and weak metal-ligand interactions as the key forces to control molecular structure, a variety of helical forming compounds can be isolated. The assembly of these compounds was monitored in the crystalline phase and shown to yield a diverse group of lattice architectures. Molecular helices have produced i) microporous networks, ii) extended helices in the lattice and iii) chiral arrays that assemble enantioselectively during crystallization. The use of C_3-symmetric compounds in supramolecular assembly is illustrated by a chiral tripodal system that forms non-centrosymmetric crystal lattices. A Ni(II)-F salt of this tripod has a lattice that is noteworthy for its six-fold symmetric open framework structure and the alignment of all the molecular Ni-F bonds along a crystallographic axis.

Keywords: *Supramolecular chemistry; hydrogen bonding; crystal engineering*

* Corresponding Author.

Comments Inorg. Chem.
2002, Vol. 23, No. 1, pp. 45-78
Reprints available directly from the publisher
Photocopying permitted by license only

INTRODUCTION

The organization of molecules into specific supramolecular assemblies in the solid state is currently an area of considerable interest in chemistry. This research generates excitement because of the possibility of incorporating well-ordered structural and functional components into a crystal lattice[1]. This can lead to the development of new materials having desirable chemical and physical properties. A variety of different synthetic methods have been reported recently which produce intricate lattice architectures[2]. All these systems rely on designed molecules to influence the assembly process. Thus the structural properties of the individual molecules are essential in the design and prediction of supramolecular assemblies. Wuest has coined the term *tecton* to describe the molecular building blocks for supramolecular assembly[3]. Tectons are molecules whose intermolecular interactions are controlled by forces allowing for specific assemblies with defined structures or functions. Organic-based tectons often use intermolecular, non-covalent interactions to assist in either self-assembly or guest-host processes[4]. These tectons are modeled usually after the complementary properties found in biomolecules. Inorganic-based tectons (metal complexes) can also be used for the formation of unique lattices: examples include coordination networks[5] and supramolecular assemblies derived from helicates[6]. These inorganic tectons often use polyfunctional organic ligands and transition metal salts to form the molecular precursor that then assembles into a supramolecular structure[5,6].

One area of this research that continues to present challenges is the prediction of the supramolecular structures (i.e., lattice architectures in crystal phases) for a given tecton. This difficulty arises because individual molecules within a lattice may adopt several different, nearly degenerate, conformations depending on the specific conditions under which the crystals are grown. For example, several factors influence assembly in inorganic tectons, such as solvent, counter-ions, and geometry of the ligands bonded to the metal ion(s). To elucidate the relationship between metal ion stereochemistry and ligand geometry in assembly processes, we have been investigating the assembly of C_2- and C_3-symmetric metal complexes[7]. These complexes contain organic molecules that have tri- or tetradentate chelates. When bonded to metal ions, these chelates can direct the assembly of supramolecular arrays in the solid state. A key component of these systems is that metal complexes are

often chiral, and thus aid in the formation of non-centrosymmetic lattices. These types of crystal lattices are a necessary prerequisite for materials having unique characteristics such as non-linear optical properties.

The general design features of our systems are shown schematically in Fig. (**1**).

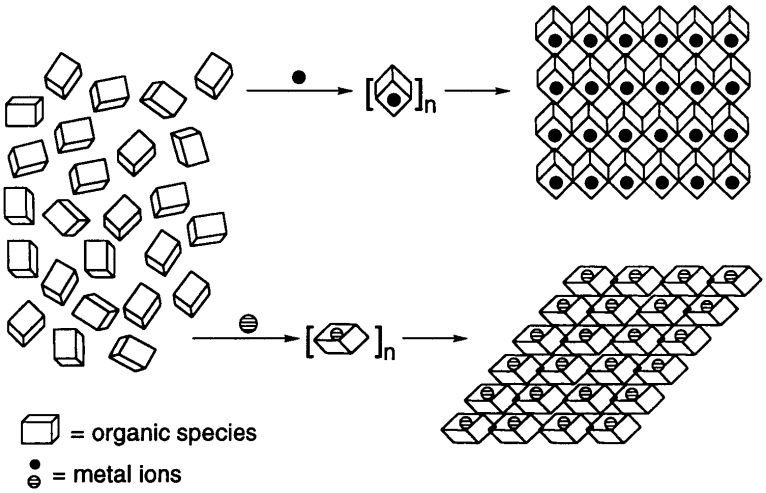

FIGURE 1 Schematic for the general approach used to make supramolecular arrays

Organic compounds are designed such that significant structural changes occur upon metal ion binding. The magnitude of these structural changes is dependent on the coordinated metal ion: metal ions with different stereochemical requirements will produce species with distinct molecular structures. This allows us to probe a variety of molecular structures either by binding different metal ions or by using metal ions that can accommodate various coordination geometries.

The assembly of the supramolecular structures is assisted by non-covalent, intermolecular interactions. Hydrogen bonding and aryl-aryl interactions are the dominant forces used in the assembly processes. These types of interactions have shown great utility in directing structural properties in synthetic and biomolecules[8]. Hydrogen bonds and

aryl-aryl interactions are weak, electrostatic interactions usually having bond energies ranging from 1 to 10 kcal/mol[8,9]. Their usefulness in structural control originates from the clustering of these interactions within a given assembled system. This effect provides significant energy of stabilization to direct the assembly process. One of the major objectives of our research is to incorporate functional groups within tectons that can orchestrate assembly of supramolecular systems through non-covalent forces.

This review summarizes our most recent studies in this area. Two types of C_2-symmetric systems are discussed: molecular helices that assemble into a variety of supramolecular arrays in the solid state. The discussion on C_3-symmetric systems emphasizes an organic tecton that assembles into chiral columns in the solid state. When coordinated to a Ni(II)-F unit, a unique non-centrosymmetric, open framework lattice is observed that has six-fold symmetry.

C_2-Symmetric Systems

Design Considerations

Fig. (**2**) shows the design factors used in developing the C_2-symmetric systems. These compounds contain a rigid 2,6-bis(carbamoyl)pyridyl unit that serves either as a site for intramolecular hydrogen bonding or a tridentate metal binding site. The metal-binding site is formed by double deprotonation of the 2,6-bis(carbamoyl)pyridyl center to afford a *meridional* chelate that becomes planar after coordination to a metal ion. This planar structure is caused by the rigidity of the 2,6-bis(carbamoyl)pyridyl chelate and is independent of the coordinated metal ion. The metallated 2,6-bis(carbamoyl)pyridyl unit has a similar function as the rigid scaffolds used by many groups in organizing peptides[10]. However, our design differs from these other scaffolds by the use of metal ions to regulate molecular structure[11]. The molecular structure in our systems is determined by the relative orientation of the groups appended from the amide nitrogens. The orientations of the appended groups are directed, to a large extent, by their interactions with the bonded metal. Each appended group is designed to contain additional donor atoms capable of binding to the metal ion. These donors are relatively weak Lewis bases whose interactions depend on the stereochemical preference of the coordinated metal ion, and *not* on the geometric requirements of the lig-

and. The coordinating donors in our systems are acyl oxygens appended from either acetophenone (H_2**1**) or amide (H_2**2**) groups. Attaching these carbonyl groups to phenyl rings allows the formation of thermodynamically favored six-membered chelate rings upon metal binding. This type of coordination results in compounds having a helical twist because both carbonyl groups can not be coplanar with the 2,6-bis(carbamoyl)pyridyl chelate.

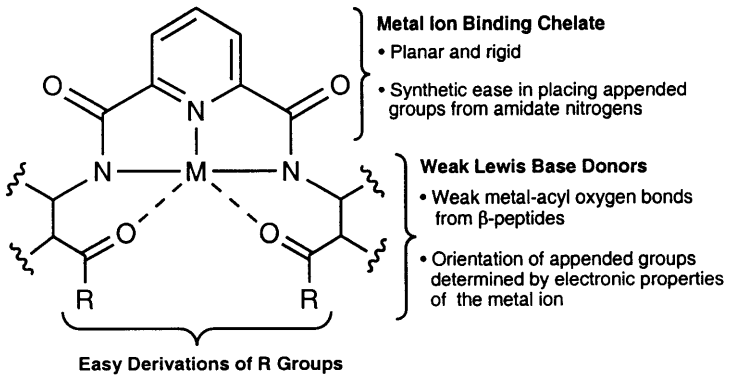

FIGURE 2 Schematic of the design concepts used in generating C_2-symmetric helices

The weak M···O=C(R) bonds are designed to influence the structures in a similar fashion as non-covalent interactions in biomolecules. For example, non-covalent interactions in protein helices allow for a variety of subtle adjustments in form which are less likely to be achieved with stronger covalent bonds[12]. By using weak M···O=C(R) bonds as a key structural element, we anticipated that a variety of molecular structures could be achieved by binding metal ions with different coordination requirements. Moreover, these differences in molecular structure between complexes should result in varied lattice architectures. This is particularly true for complexes containing divalent metal ions that will be electronically neutral. To investigate the usefulness of this approach, we studied the solution and solid state structures of Ni**1** and Cu**1**. These studies will demonstrate that M···O=C(R) bonds are indeed weak interactions and significant lattice changes can occur with only minor molec-

ular changes. The design concept is further developed with the β-peptide compound H_2**2**. Systems derived from this compound show that chiral resolution can be obtained during crystal growth.

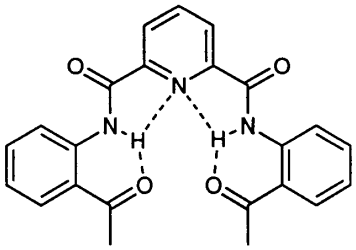

H_2**1**

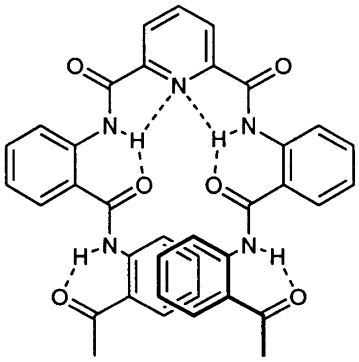

H_2**2**

Solution Properties Ni1

The ^{1}H NMR spectrum of the diamagnetic Ni**1** complex contains six distinct aryl signals and one acyl methyl peak; this result is consistent with a symmetrical coordination of $[\mathbf{1}]^{2-}$ about the Ni(II) ion. This symmetrical interaction mandates tridentate coordination between the Ni(II) and the 2,6-bis(carbamoyl)pyridyl binding pocket. Because the binding pocket does not complete the inner coordination sphere about the Ni(II) ion, the acyl oxygens of the appended acetophenone groups also interact symmetrically with the Ni(II) center. These Ni···O=C(Ph) interaction(s) should influence the proton chemical shifts of the supporting phenyl groups, such as is seen for the protons ortho to the amide nitrogens (H_a) whose chemical shift is observed at 8.29 ppm. The downfield proton chemical shift of H_a is caused by a deshielding effect from the amide carbonyl groups of the planar 2,6-bis(carbamoyl)pyridyl binding pocket. For this deshielding to occur the dominant conformation of the appended acetophenone moieties is one that has the phenyl rings nearly coplanar with the Ni(II)-2,6-bis(carbamoyl)pyridyl unit. This agrees with molecular models that predict that a Ni···O=C(Ph) interaction requires nearly coplanar conformations between the appended groups

and the metal binding pocket. Finally, we have observed a positive NOE between H_d (phenyl protons ortho to the carboryl groups) and the acetyl methyl protons, indicating that the appended carbonyl oxygens are oriented towards the bound Ni(II).

Structural information for Ni**1** and Cu**1** in solution was also obtained from FTIR measurements. The FTIR spectrum of Ni**1** in CH_2Cl_2 contains two acetophenone carbonyl stretches at 1680 and 1653 cm^{-1}, whereas Cu**1** has only one signal at a frequency of 1627 cm^{-1}. The lowering of the ketone stretching frequency from 1684 cm^{-1} (ν_{CO} for acetophenone) to 1653 and 1627 cm^{-1} in Ni**1** and Cu**1** respectively, is expected for an acyl oxygen interacting weakly with a metal center. These shifts to lower energy are comparable to those found for carbonyl oxygens involved in hydrogen bonding[13]. Furthermore, these results suggest that Cu**1** and Ni**1** have different molecular structures, with Cu**1** favoring a symmetric five-coordinate species while Ni**1** has an unsymmetrical four-coordinate structure. A conformational equilibrium for Ni**1** that is consistent with the results from NMR and FTIR spectroscopies is shown in eq 1. Each four-coordinate Ni**1a** and Ni**1b** species has only one Ni···O=C(Ph) interactionwhich yields the two unsymmetrical square planar complexes. This equilibrium is rapid compared to the NMR timescale (even at −60°C) and prevents us from observing these individual species, as seen from the symmetrical spectrum for Ni**1**, but can be resolved in the FTIR spectrum.

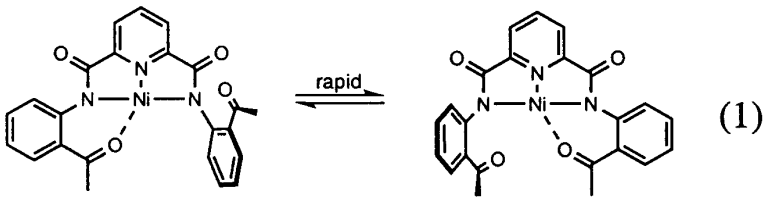

Ni**1a** Ni**1b** (1)

Molecular Structures

The molecular structures of Ni**1** and Cu**1** agree qualitatively with the picture that emerged from our spectroscopic studies in solution. Both complexes have three of their coordination sites occupied by nitrogen donors from the 2,6-bis(carbamoyl)pyridyl chelate. In Ni**1** the geometry

around the Ni(II) is approximately square planar, with the fourth donor provided by a carbonyl oxygen, O(4), from one of the appended acetophenone groups. The acyl oxygen coordination orients this group nearly coplanar with the rigid, tridentate chelate. The remaining acetophenone oxygen O(3) is pointed away from the Ni(II) center at a distance of ~ 5.5 Å (*vide infra*).

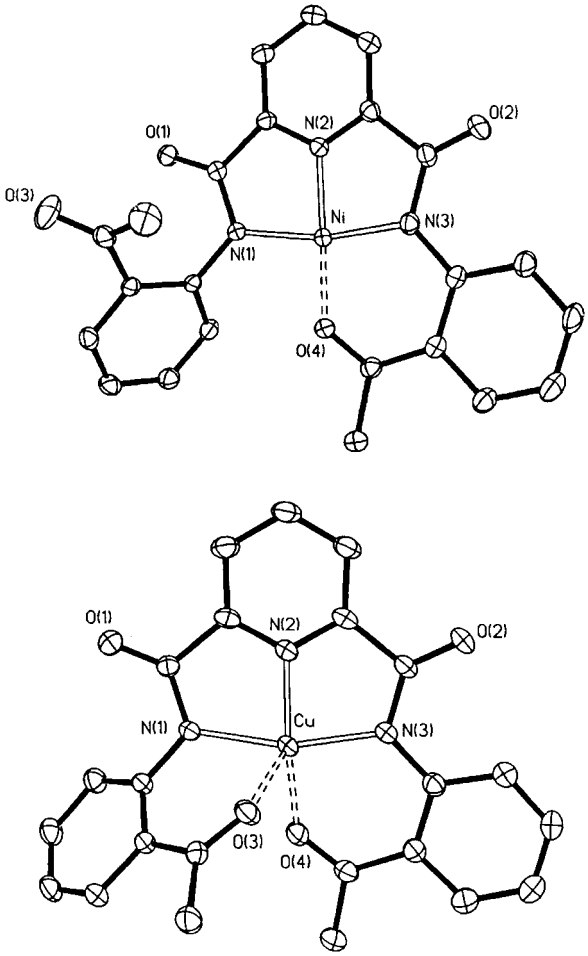

FIGURE 3 Thermal ellipsoid diagrams of Ni**1 (A)** and Cu**1 (B)**. The ellipsoids are drawn at the 40% probability level and hydrogens are removed for clarity

In contrast to Ni**1**, both acetophenone oxygens in Cu**1** interact with the copper(II) center producing a square pyramidal five-coordinate species with O(3) occupying the axial position. These oxygen donors are coordinated unsymmetrically to Cu(II), with distances of 2.357(3) and 1.933(3) Å for the Cu-O(3) and Cu-O(4) bonds respectively. Dual coordination of carbonyl oxygens causes the appended acetophenone groups to orient on opposite faces of the plane formed by the Cu(II)-[2,6-bis(carbamoyl)pyridyl] unit. The structural consequence of this displacement gives Cu**1** an overall helical morphology[14].

The solid state molecular structures of Ni**1** and Cu**1** also allowed us to further probe the nature of the M···O=C(Ph) interaction. The Ni-O(4) and Cu-O(4) bond distances of 1.828(3) and 1.932(3) Å are suggestive of relatively strong equatorial M-O interactions present in these compounds. However, molecular modeling studies show that for equatorial coordination of an acyl oxygen to the M(II)-[2,6-bis(carbamoyl)pyridyl] unit, the oxygen donor must reside ca. 1.9 Å from the bound metal center. This inflexibility in the ligand system restricts all near-planar metal-carbonyl oxygen interaction(s); thus we propose that these short bond lengths in Cu**1** and Ni**1** are actually caused by the structural constraints imposed by $[\mathbf{1}]^{2-}$. This hypothesis is supported by two lines of structural evidence in Ni**1** which show that the Ni-O(4) interaction is indeed weak. First, the Ni-N(2) bond distance of 1.805 (2) Å is exceptionally short compared to known pyridine nitrogen-nickel bonds incorporated into two five-membered ring metallocycles (>1.95 Å).[15] This short bond length is consistent with a weak *trans* influence of the O(4) with the Ni center. Secondly, the C(22)-O(4) bond length of 1.260 (4) Å is only slightly longer than that normally observed for a C=O bond (1.23 Å) but is still much shorter than the distance for a C-O single bond (1.43 Å)[16]. This minor elongation of the C=O bond reflects the small decrease in the carbonyl bond order that occurs from the M···O=C(Ph) interaction which agrees with our FTIR measurements (*vide supra*).

Comparison of Molecular Structures of Ni1 and Cu1

An overlay of the two molecular structures (Fig. (**4**)) reveals that the complexes have a strong structural similarity through the coordination square plane (RMS = 0.10 Å). The only difference between the two structures is in the position of the appended acetophenone group containing O(3). This acetophenone group in Ni**1**is nearly coplanar to the

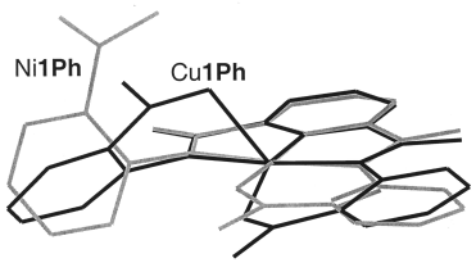

FIGURE 4 Overlay of the molecular structures of Ni**1** and Cu**1**

2,6-bis(carbamoyl)pyridyl chelate with a dihedral angle of 3.8° observed between the plane formed by the chelate and the aryl ring of the appended acetophenone group. The corresponding dihedral angle in Cu**1** is 12.5°. The major difference between the molecular structures of Ni**1** and Cu**1** is the orientation of the acetophenone groups containing O(3). In Ni**1**, this group is oriented such that the aryl ring is rotated 118.5° out of the coordination square plane. The acetyl oxygen O(3) is pointed away from the Ni(II) center and is hydrogen bonded to one solvated water molecule. However in Cu**1**, where O(3) is coordinated to the Cu(II) center, this appended group is displaced only 48° from the plane of the 2,6-bis(carbamoyl)pyridyl chelate. This structural difference has a significant influence on the assembly of the complexes in their respective crystal lattices.

Lattice Structures for Cu1 and Ni1

As shown in Fig. (**5**), there are three principal intermolecular interactions between complexes in the lattice of Cu**1**. The complexes are arranged such that the aryl rings of $[\mathbf{1}]^{2-}$ in one complex are π-stacked with the corresponding rings of neighboring complexes[17]. Hence, π-stacking interactions between pyridyl rings are found at a centroid-centroid distance of 3.92 Å and at 4.45 Å for the aryl rings from the equatorial coordinated acetophenones. These two interactions support the arrangement of Cu**1** complexes into coils that are aligned along the crystallographic *b*-axis. Adjacent coils interact *via* π-stacking interactions between the aryl rings of the apically coordinated acetophenone

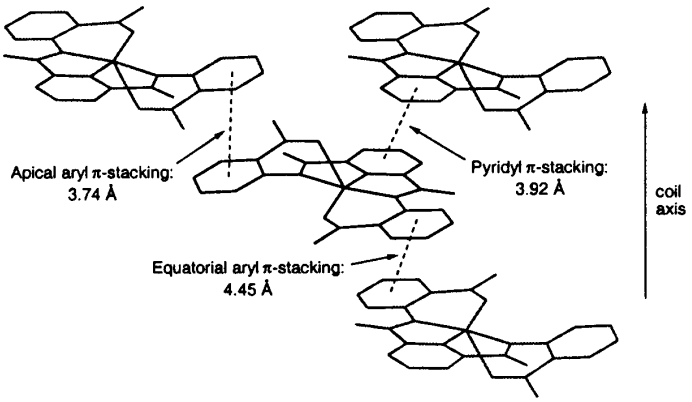

FIGURE 5 Intermolecular π-stacking interactions observed in the lattice of Cu**1**

groups (i.e., the appended group containing O(3)) with a centroid-centroid distance of 3.74 Å.

An open-framework lattice results (Fig. (**6**)) where the distance between adjacent set of stack rings is 7.74 Å. This space in the present structure of Cu**1** is filled with toluene molecules that come from the solvent used in crystallization.

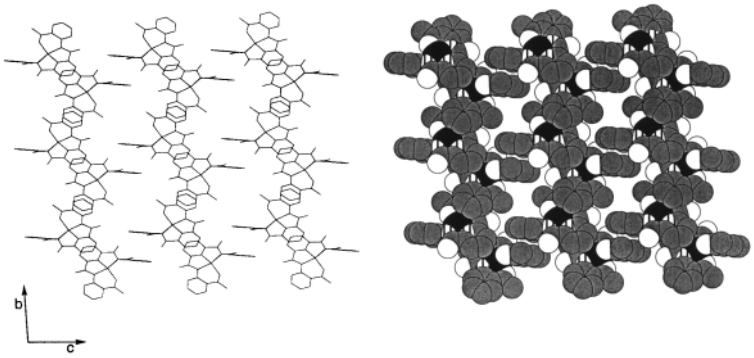

FIGURE 6 A portion of the crystal lattice for Cu**1** (view of the *b,c* plane). Solvent molecules have been omitted for clarity

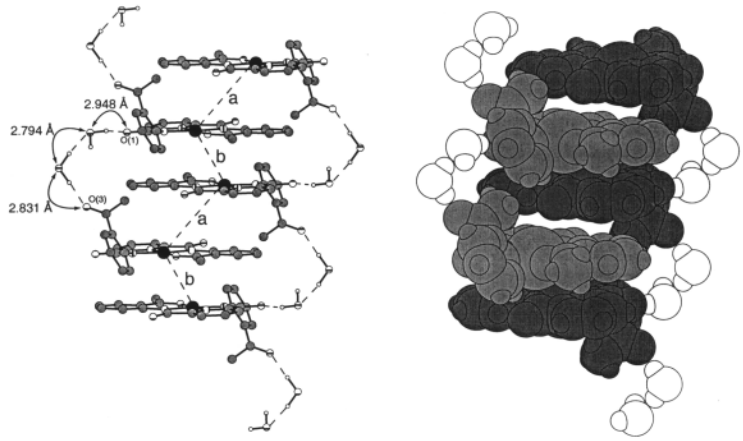

FIGURE 7 A portion of the crystal lattice for Ni**1** illustrating the hydrogen bonding network used to stabilize the column motifs. Intra-columnar Ni-Ni distances: *a*, 4.42 Å and *b*, 6.21 Å

Fig. (**7**) shows that Ni**1** complexes assemble into supramolecular columns that are positioned along the crystallographic *b*-axis. The columns are stabilized through two hydrogen bond networks that are on opposite sides of each column. The hydrogen bond networks connect every other complex through repeated units consisting of two hydrogen bonded water molecules. These pairs of water molecules in turn hydrogen bond to O(3) of an appended acetophenone group from one complex and O(1) of a 2,6-bis(carbamoyl)pyridyl chelate of an alternating complex. Additional columnar stabilization comes from stacking interactions between the coordination square planes of adjacent molecules where the average inter-plane distance is 3.75 Å. This arrangement of Ni**1** complexes results in two unique intra-columnar Ni-Ni distances at 4.42 Å and 6.21 Å. The dominant inter-columnar forces are edge-to-face interactions between molecules in adjacent columns that are aligned along the crystallographic *c*-axis: these weak aryl interactions occur between the appended acetophenone groups that contain O(3) where the centroid-centroid distance is 4.88 Å. This arrangement of columns within the lattice produces extended hydrophilic channels that are filled with water molecules (Fig. (**8**)).

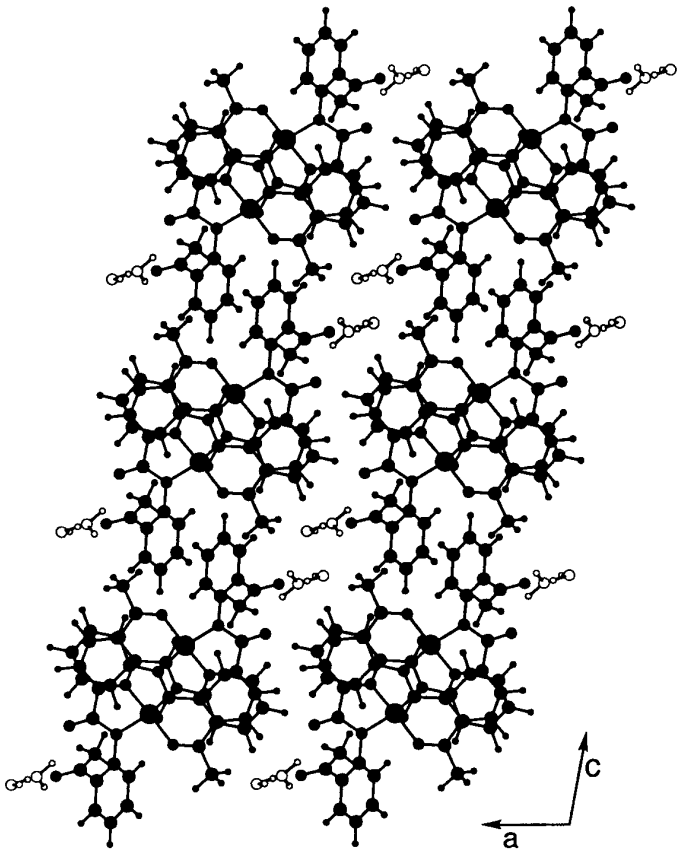

FIGURE 8 Portion of the crystal lattice for Ni**1** (view of the *a*,*c* plane) showing the intermolecular column interactions and the resulting water filled channels

Helical Tectons: Structure of $H_2$2

The results obtained with Ni1 and Cu1 show that our design yields compounds that serve as building blocks to assemble varied supramolecular structures in the solid state. The use of relatively weak M···O=C(R) interactions allows for diverse molecular structures which affects

supramolecular assembly. To further explore these concepts in the assembly of supramolecular arrays, we investigated the structural properties of H_2**2**. This compound has appended groups that contain β-peptides: each appendage contains two aryl rings connected by amide linkages. The increase in aryl groups affects assembly by increasing the number of possible aryl-aryl interactions within a supramolecular array. It should be noted that a similar design strategy to that of H_2**2** has been reported by Hamilton and coworkers, although they have not reported the effects of metal binding on helicity[18].

H_2**2** contains two preorganized aryl appendages that are self-assembled through hydrogen bonds and tethered covalently to the 2,6-bis(carbamoyl)pyridyl template. As described in the design section, this compound will have an inherent helical twist that is stabilized by bifurcated hydrogen bonding between the pyridyl nitrogen, the amide protons (H_a), and the adjacent acyl oxygens of the appendages. This intramolecular hydrogen bonding is indicated from the ^{1}H NMR spectrum of H_2**2** in $CDCl_3$ that shows that the amide protons H_a and H_b have large down-field chemical shifts (Fig. (**9**)). These hydrogen bonds restrict the orientation of the aryl rings within the appended arrays as shown by the strong intra-array NOEs observed between H_b and H_h of the neighboring phenyl ring and between H_l and the methyl protons of the terminal ketone (H_m). In the solid state, H_2**2** has a helical structure, which largely results from bifurcated hydrogen bonds between the pyridyl nitrogen, the amide protons (H_a), and the adjacent acyl oxygens (O(2) and O(5)) of the appendages. The appendages cross with a stacking distance of 3.27 Å (Fig. (**9**)).

The effects of metal binding on the structure of H_2**2** was probed by examining the structural properties of Ni**2** and Cu**2**. The ^{1}H NMR spectrum of the Ni**2** complex contains one acyl methyl and 10 aryl signals. This result is consistent with a symmetrical coordination of $[\mathbf{2}]^{2-}$ about the Ni(II) ion- a result that is similar to that observed in our other Ni(II) system, Ni**1** (*vide infra*). The large downfield shift of the amide protons (H_b) at 13.01 ppm shows that intramolecular hydrogen bonding is maintained within the appended groups[13]. Moreover Ni**2** has NOEs analogous to those observed for H_2**2**. These results show the significant effect that the hydrogen bonds impart on the conformation of the appended arrays in Ni**2**; restricting the aryl rings in an *anti* orientation about the amide bond.

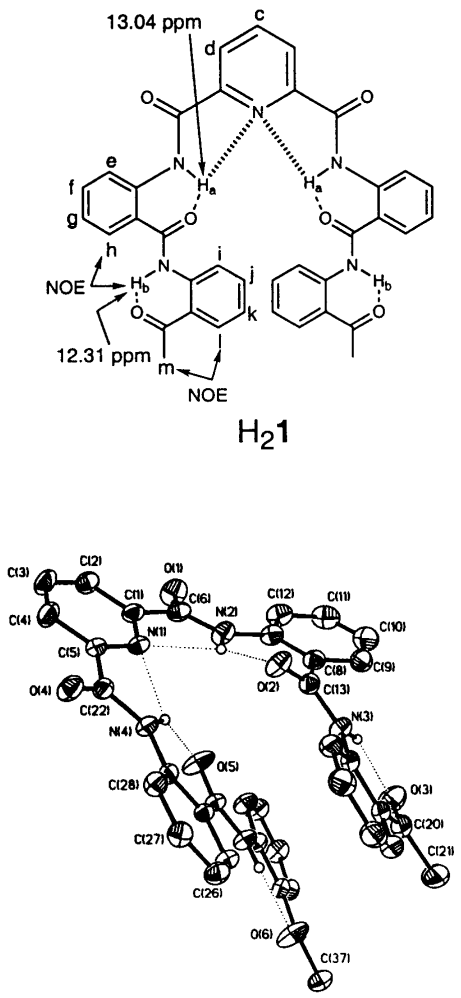

FIGURE 9 A structural scheme of H_2**2** showing selected NMR data (left) and a thermal ellipsoid diagram of H_2**2** (right) with ellipsoids drawn at the 50% probability level. Non-amide hydrogens are removed for clarity

Ni**2** exists as a racemic mixture of left- and right-handed enantiomers in solution that are slow to exchange on the NMR timescale. This is

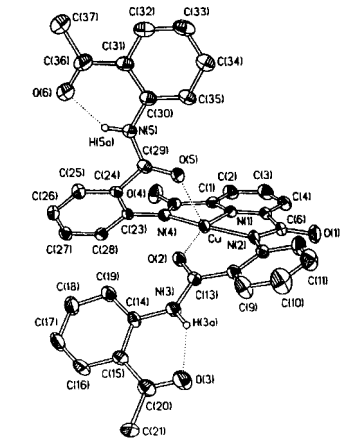

Cu2g$_p$

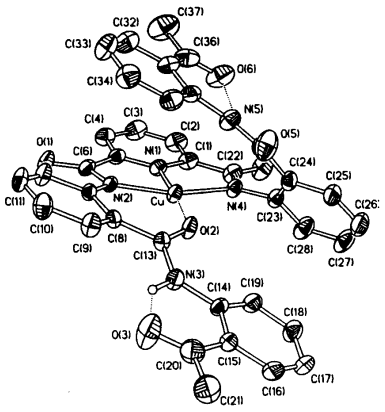

Cu2r

FIGURE 10 Thermal ellipsoid diagrams of Cu**2gP (A)** and Cu**2r (B)**. Ellipsoids are drawn at the 50% probability level. The solvent molecules and non-amide hydrogens are removed for clarity

demonstrated by treating a $CDCl_3$ solution of Ni**2** with Pirkle's reagent, [(*S*)-(+)-trifluoro-1-(9-anthryl)ethanol][19]. An upfield shift and doubling of the proton signals are observed upon addition of the chiral solvating reagent, consistent with the presence of a pair of diastereomeric adducts. In contrast, H_2**2** does not show this resolution with Pirkle's reagent illustrating the importance of the metal ion in maintaining helical morphology.

Attempts to obtain single crystals of Ni**2** were unsuccessful. However, Cu**2** readily yielded crystals that were suitable for X-ray diffraction studies; Cu**2** confirms that helicity is preserved in the solid state. Cu**2** crystallizes initially in the centrosymmetric space group $P\bar{1}$ as green blocks having a molecular structure composed of two crystallographically independent chiral molecules (Cu$\mathbf{2g_P}$ and Cu$\mathbf{2g_M}$). The chirality observed in Cu$\mathbf{2g_P}$ and Cu$\mathbf{2g_M}$ arises from their helical form, with Cu$\mathbf{2g_P}$ having a right-handed helix and Cu$\mathbf{2g_M}$ a left-handed one (the subscripts, P and M denote the right and left-handed conformations of the helix)[20]. The molecular structure of Cu$\mathbf{2g_P}$ is shown in Fig. (**10a**).

TABLE I Selected Structural Parameters for H_2**2**, Cu**2g** and Cu**2r**

Distances (Å) and angles (°)	*H_2**1***	*Cu**1g**$_P$*	*Cu**1g**$_M$*	*Cu**1r***
p[a]	4.190	7.613	7.413	6.168
r[a]	3.140[b]	3.192	3.412	2.453
ø(*ø′*)[a]	–1.8°(-1.5°)	0.0 (5.3)	–1.6(7.3)	–2.8 (-1.0)

a. *ø* is described by N(2)-C(7)-C(8)-C(13), *ø′* by N(4)-C(23)-C(24)-C(29). Pitch of the helix is the distance (Å) from C(14) to C(30). Radius of helix is the distance (Å) of the line from the Cu(II) center perpendicular to the pitch line.
b. Radius in H_2**2** is measured from the centroid of N(5), N(4), O(2), and O(5).

These molecules have nearly identical square pyramidal coordination geometry about the copper(II) ion; three nitrogen donors are provided by the rigid 2,6-bis(carbamoyl)pyridyl template with additional ligation supplied by the two adjacent amide oxygens of the appendages. The H-bonded appendages are held rigid by intramolecular hydrogen bonding, with the aryl rings in a slightly twisted *anti* alignment around the amide bond. The helical morphologies of the complexes are clearly determined by the interactions of the arrays with the metal template via

the Cu-O bonds. For example, the helices in Cu**2g$_P$** and Cu**2g$_M$** have a pronounced unsymmetrical twist, as is evident by the nonequivalent torsional angles (ø and ø′) found for each molecule (Table I). This asymmetry is caused by the large difference between the Cu-O(5) and Cu-O(2) bond lengths which leads to unsymmetrical orientation of the appended arrays about the metal template.

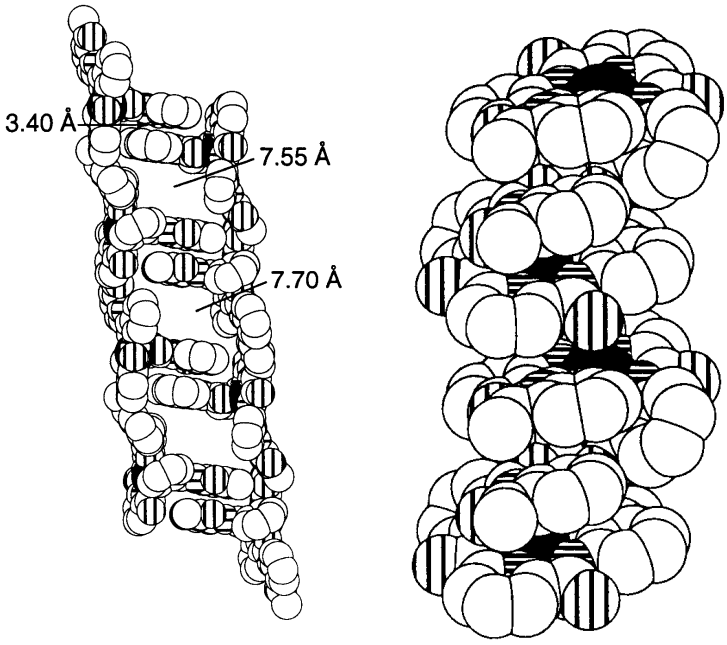

FIGURE 11 Space-filling representations for a portion of the crystal lattice in Cu**2g** (viewed along b-c plane) illustrating the microporous motif (**A**), and Cu**2r** (aligned along a-axis) showing the intermolecular helix (**B**). The solvent molecules and non-amide hydrogens are removed for clarity

Cu**2** provides an opportunity to examine how coordination changes at the metal center alter morphology. Over a period of several weeks, the crystalline five-coordinate green complex changes to a red species (Cu**2r**) whose molecular structure is depicted in Fig. (**10b**). The molecular basis for the color change is the absence of the weak axial Cu-O(5)

interaction in Cu**2r**, leaving this complex with a four-coordinate copper(II) center. This single reduction in coordination at the metal results in a major structural rearrangement of the helix. The amide oxygen O(5), which is axially coordinated to Cu(II) in the green form, is rotated away from the metal template in Cu**2r**, causing most of the axial appended groups to be poised within van der Waals contacts of the metal template. This realignment of the axial appendage (the one that contains O(5), see Fig. (**10**)) produces a much smaller helix compared to those found in the green form. For example, the pitch (*p*) in Cu**2r** is smaller by 1.445 Å than that found in Cu**2r** and the radius (*r*) has decreased by 0.739 Å. Moreover, the helix in Cu**2r** has similar torsional angles of –2.8° and –1.0° (Table I).

The variance in structure between the green and red forms of Cu**2** is amplified in the crystal lattice. The lattice of Cu**1g** has an open-framwork (Fig. (**11a**)); the pores are formed *via* parallel aryl ring π stacking between the axial appendages of Cu$\mathbf{2g_P}$ and Cu$\mathbf{2g_M}$ (the aryl-aryl stacking distance is 3.40 Å). The space between adjacent sets of stacked rings (~7.60 Å) contains two disordered toluene molecules. In contrast, the helical molecules of Cu**1r** associate to form longer, extended helices in the solid state (Fig. **11b**). Each extended helix consists of alternating right- and left-handed helical monomers that assemble through intermolecular π-stacking interactions. Within an extended helix, two intermolecular Cu-Cu distances (5.504 Å and 9.131 Å) are observed between a Cu(II) monomer and its nearest neighbors. This close arrangement of molecules in the lattice of Cu**1r** yields crystals that are significantly more dense than those found for the porous Cu**1g** isomer (Cu**1r**, 1.505 g/cm^3; Cu**1g**, 1.137 g/cm^3). The structural properties of Cu**2r** appear to be present only in the crystalline state; dissolution of the red crystals in toluene or CH_2Cl_2 produces green solutions that have spectroscopic properties identical to those found for Cu**2g**.

Chiral Resolution During Crystal Growth: Cu2(py)

The results of H_2**2**, Ni**2**, and Cu**2** showed that these helical compounds are useful in assembling new supramolecular structures. However, in both solution and the solid state they exist as racemic mixtures of left-handed and right-handed helices. Clearly, an exciting application of these systems is to use their intrinsic chirality to form chiral supramolecular arrays. Insight into how this might be accomplished came from a

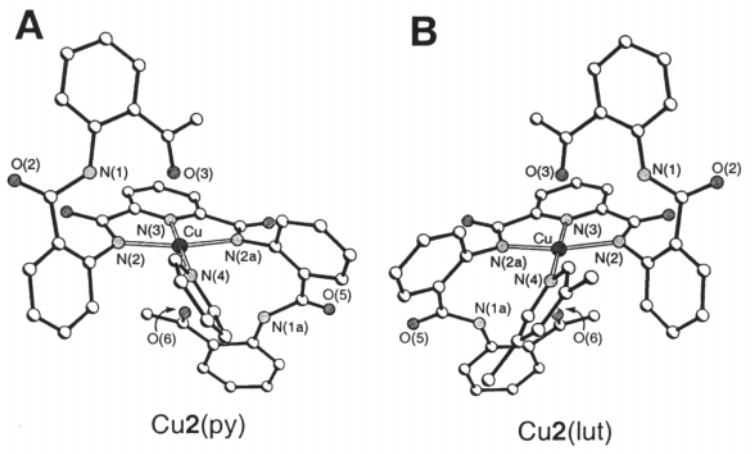

FIGURE 12 Thermal ellipsoid diagrams of Cu**2**(py) (**A**) and Cu**2**(lut) (**B**). Hydrogens are removed for clarity

further analysis of the structure of the five-coordinate Cu**2g** compound. The coordination sphere of the Cu(II) center is provided by three nitrogen donors from the 2,6-bis(carbamoyl)pyridyl chelate and two inner amide oxygens (O(2), O(5)) of the appended aryl groups. The Cu···O_{amide} interactions are significant in determining the helical morphology; the unsymmetrical helix in Cu**2g** results from different Cu-O_{amide} bond distances (Cu···O(2), 1.931 (4); Cu···O(5), 2.315 (4) Å).

This analysis on Cu**2g** suggested that modifications in helicity can occur by breaking either one or both of the structurally important Cu···O_{amide} bonds. Since these bonds are relatively weak, the O_{amide} donors should be readily substituted by more basic exogenous ligands. Substitution can indeed happen when Cu**2** is treated with pyridine ligands. Dissolving Cu**2** in neat pyridine changes the electronic absorption and EPR spectroscopic properties of the complex indicating that the coordination environment about the Cu(II) center has been altered.

Crystallization of Cu**2**(py) produces crystals having diamond morphology. X-ray diffraction studies on Cu**2**(py) confirms that binding of a single pyridine to copper causes a significant structural rearrangement. The molecular structure of Cu**2**(py) is presented in Fig. (**12**). The copper

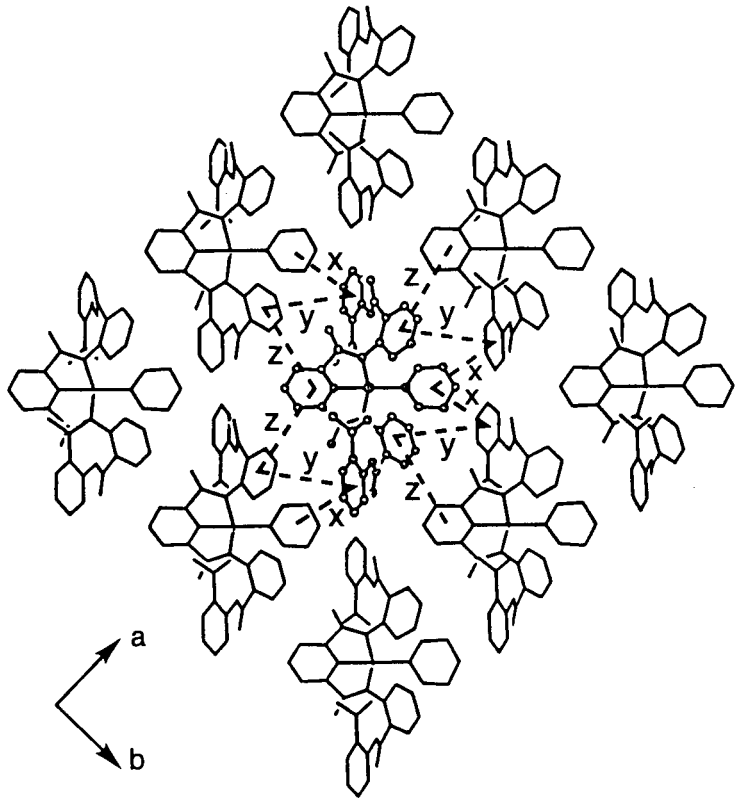

FIGURE 13 A portion of the crystal lattice for Cu**2**(py) (view of *a*,*b* plane). Selected intermolecular aromatic centroid-centroid distances (Å) [and corresponding interplane angles (°)]: x, 4.98 [64.5]; y, 5.10 [70.7]; z, 5.86, [62.7]

in Cu**2**(py) is bound by a pseudo-square planar arrangement of nitrogen atoms provided by the 2,6-bis(carbamoyl)pyridyl chelate and the exogenous pyridine. Nitrogen atom N(4) of the exogenous pyridine is positioned *trans* to the pyridyl nitrogen N(3) of $\mathbf{2}^{2-}$. The Cu**2**(py) complex has exact C_2 symmetry where the axis bisects the two pyridine rings, coinciding with atoms N(3), Cu and N(4). The two O_{amide} donors that were coordinated originally to the copper in Cu**2** (O(2) and O(5)) are rotated away from the copper in Cu**1**(py) and no longer interact with the

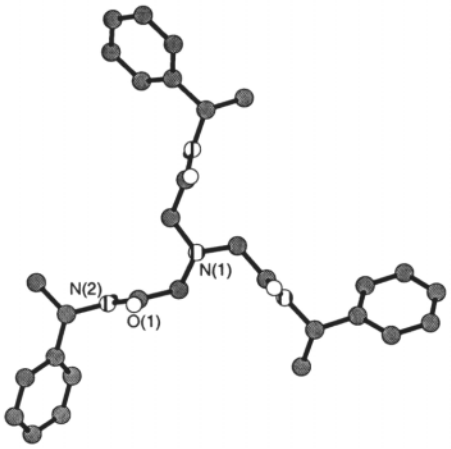

FIGURE 14 View of the molecular structure of $H_3\mathbf{3}^{S-mbz}$ illustrating the C_3 rotational symmetry of the molecule

metal ion (Cu···O(2) distance is 5.89Å). A chiral cleft about the exogenous pyridine is formed by the appended groups in $[\mathbf{2}]^{2-}$. The inner aryl moieties of the appended groups are intramolecularly π-stacked with the bound pyridine at $centroid_{aryl}$-$centroid_{py}$ distances of 4.37 Å and all three rings are canted in the same direction relative to the planar 2,6-bis(carbamoyl)pyridyl chelate (average angle between ring planes and the chelate is −57°). The outer aryl rings of the appendages are positioned above and below the equatorial coordination plane with the acetophenone oxygens O(3) and O(6) located 2.618 (9) Å from the copper(II) center.

The difference in the molecular structure of Cu**2**(py) from that of Cu**2** correlates with large changes in their lattice architectures. The crystal structure of Cu**2**(py) shows that *chiral* assembly has occurred where all the compounds within the lattice have the same helical chirality. Since NMR studies show that $H_2\mathbf{2}$ is achiral in solution (*vide supra*), the observed helicity in Cu**2**(py) must result from spontaneous resolution as individual crystals form. Crystallization from solution should produce enantiomeric crystals in equal numbers. A crystal of the other handed-

ness has been characterized for Cu**2**(lut); this diamond shape crystal belongs to the tetragonal space group $P4_32_12$, the enantiomorph of the $P4_12_12$ space group found for Cu**2**(py). The crystal lattices of the two structures are almost identical with only slight deviations (< 8%) observed in their unit cell parameters. Moreover, the molecular structure of Cu**2**(lut) is similar to that described above for Cu**2**(py), the major difference being the opposite helicity (Fig. (**12**)).

An explanation into the observed chiral resolution comes from the similar lattice architecture shared by Cu**2**(py) and Cu**2**(lut). The lattices contain ordered arrays of helices in the *a*,*b* plane. Each helix is positioned at the center of a hexagon composed of six surrounding helices; between neighboring helices there are twelve edge-to-face aromatic interactions. Three of these interactions are unique by symmetry, which for Cu**2**(py) are at aryl ring centroid-centroid distances of 4.98, 5.10, and 5.86 Å with corresponding interplane angles of 64.5, 70.7, and 62.7° (Fig. (**13**). For Cu**1**(lut), two unique edge-on interactions are observed at centroid-centroid distances of 5.39 and 6.30 Å. Four weak methyl-aryl interactions between the methyl groups of the coordinated lutidine and the aromatic rings of neighboring helices are also observed at distances of 4.07 Å. The clustering of weak edge-on interactions within an array undoubtedly contributes to the stabilization of these supramolecular assemblies of helices[8,21] Edge-on interactions are weakly electrostatic and depend on the orientation of the two aryl rings. Theoretical investigations suggest that attractive edge-on interactions similar to those observed in Cu**2**(py) and Cu**2**(lut) can contribute between 0.5–2 kcal/mol (per interaction) to the stabilization of a structural motif[8]. This type of stabilization necessitates the nearly perfect alignment of helices within an array that is only possible if individual helices are of the same helicity. Thus the assembly of the arrays during crystallization is enantioselective for one helicity.

C_3-Symmetric Systems

Design Considerations

We have also designed a new series of C_3-symmetric compounds based on a tripodal arrangement of functional groups. The tripodal character of these compounds arises from the three carbamoylmethyl arms surrounding a central amine nitrogen. We have synthesized a homochiral

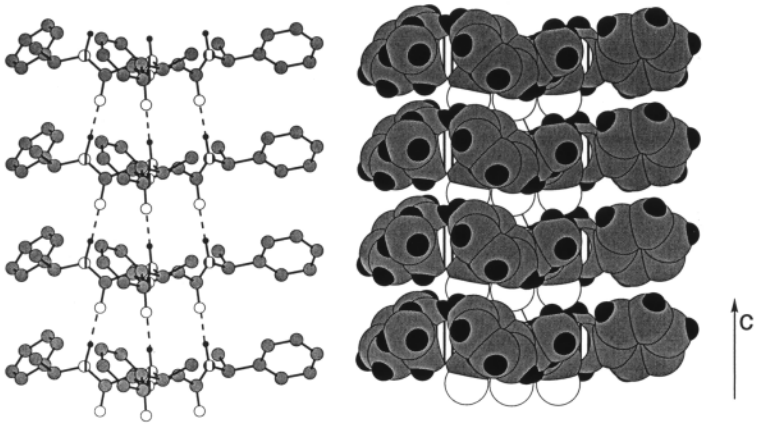

FIGURE 15 A portion of the crystal lattice for $H_3\mathbf{3}^{S-mbz}$ (view of the *b,c* plane) showing the column motif

analog ($H_3\mathbf{3}^{S-mbz}$) by placing optically pure (*S*)-(-)-(α)-methylbenzyl groups at the ends of each tripodal arm *via* linkages to the amide nitrogens[22,23]. It was anticipated that the placement of these chiral groups next to the amide moieties, which have the potential to hydrogen bond, would influence the assembly of the crystal lattice. Thus, the self-complementary[24] character of this compound would control its assembly into aggregates *via* both intermolecular hydrogen bonds and edge-to-face aryl interactions.

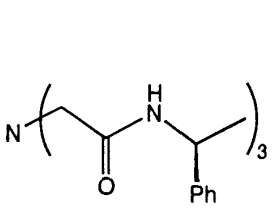

$H_3\mathbf{3}^{S-mbz}$

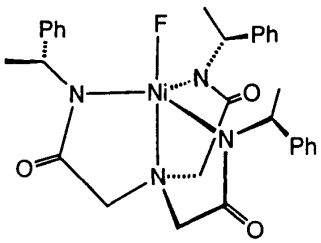

$[Ni\mathbf{3}^{S-mbz}(F)]^{2-}$

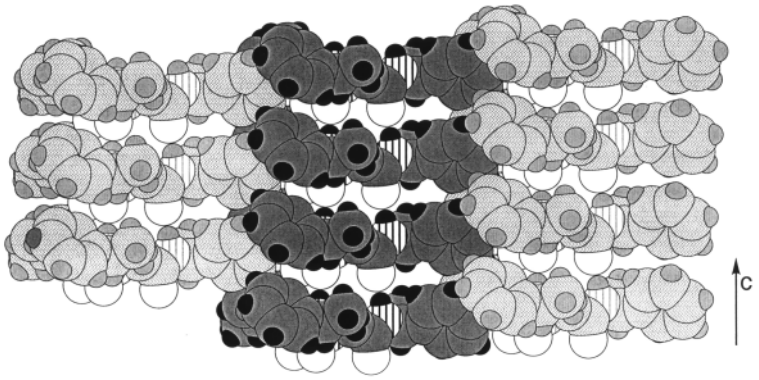

FIGURE 16 The crystal structure of $H_3\mathbf{3}^{S-mbz}$ showing the intercolumn interactions within the crystal lattice (view of the *b*,*c*plane)

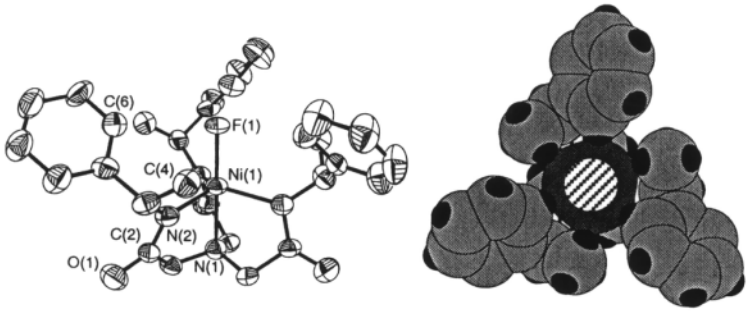

FIGURE 17 Thermal ellipsoid diagram of $[Ni\mathbf{3}^{S-mbz}(F)]^{2-}$ and a space-filling representation of the complex. The ellipsoids are drawn at the 40% probability level and hydrogens are omitted for clarity. Selected bond distances (Å) and angles (°): Ni(1)-F(1) = 1.950 (6); Ni(1)-N(1) = 2.104 (10); Ni(1)-N(2) = 2.073 (4); C(6)-F(1) = 3.165; N(1)-Ni(1)-F(1) = 180.000 (2); N(2)-Ni(1)-F(1) = 100.86 (11); N(2)-Ni(1)-N(1) = 79.15 (11); N(2)-Ni(1)-N(2) = 116.54

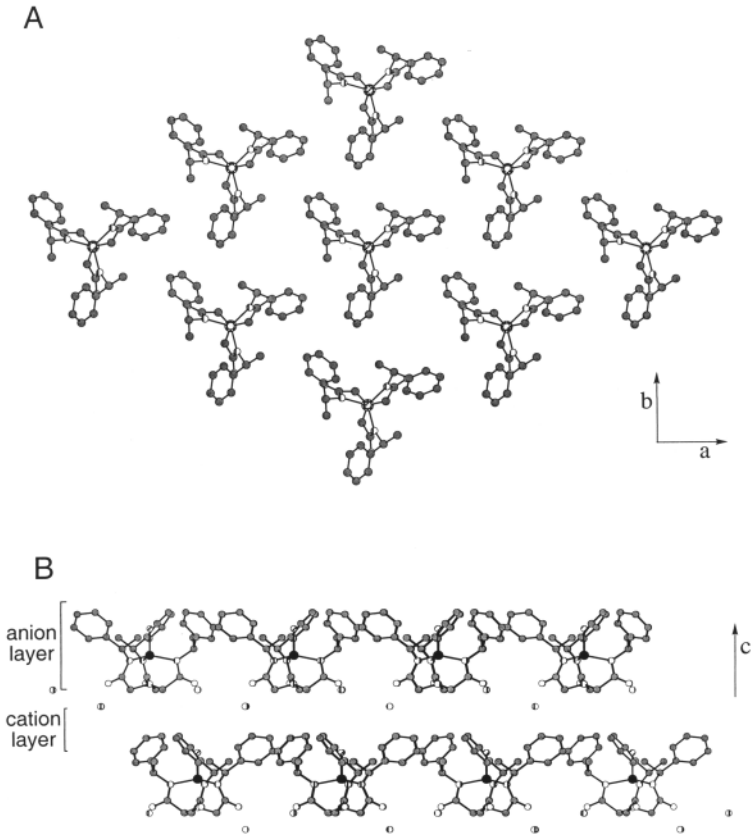

FIGURE 18 A portion of the crystal lattice for [Ni**3**$^{S-mbz}$(F)]$^{2-}$ (**A**) (viewed along the *a*,*b* plane and (**B**) (viewed along the *b*, *c* plane) showing the positions of the nitrogen atoms of the Et_4N^+ ions. Hydrogens have been omitted for clarity

*Solid State Structure of H_3**3**$^{S-mbz}$*

Crystallization of H_3**3**$^{S-mbz}$ resulted in colorless sheet-like crystals belonging to the non-centrosymmetric space group *R*3. A representation of the molecular structure of H_3**3**$^{S-mbz}$ is located in Fig. (**14**). Each H_3**3**$^{S-mbz}$ molecule sits on a crystallographic three-fold axis where the

three tripodal arms are symmetrically positioned around the central amine nitrogen. The three amide moieties in each molecule of H_3**3**$^{S\text{–mbz}}$ are oriented such that the carbonyl groups are on one molecular face with the NH bonds positioned on the opposite face. The radially symmetric orientation of amide groups produces supramolecular C_3-symmetric columns that are aligned parallel with the crystallographic *c*-axis. Each column is stabilized by a network of hydrogen bonds where individual molecules in a column participate in six intermolecular hydrogen bonds, three to each of its nearest neighbors (Fig. (**15**)). The positioning of H_3**3**$^{S\text{–mbz}}$ molecules within a column is ideal for the formation of intermolecular hydrogen bonds as is indicated by the short N···O distance of 2.846 Å and the nearly linear N-H-O angle of 179.4°. In addition, an individual molecule is involved in three aryl-aryl stacking interactions with each adjacent molecule within a column. The aryl rings of the methylbenzyl groups of the tripodal arms have π-π stacking interactions at a distance of 4.887 Å (centroid-to-centroid) causing the stacked rings to have identical orientations (Fig. (**15**)).

Inter-columnar stabilization is dominated by edge-to-face aryl and methyl-to-aryl interactions. Every column is surrounded by six other columns, three of which are in-register and three columns are out-of-register, offset by one-third of a unit cell as required by the *R*3 crystal symmetry (Fig. (**16**)). This ordering results in each tripodal arm of an individual molecule within a column having two edge-to-face aryl interactions with molecules of adjacent columns where the aryl centroid-centroid distances are 5.397 and 6.089 Å[8,22]. In addition, two inter-column methyl to aryl interactions per tripodal arm are observed at distances of 4.448 and 5.145 Å (methyl carbon to aryl centroid).

The columnar motif found in the crystal lattice of H_3**3**$^{S\text{–mbz}}$ resembles that found by Hamilton and coworkers for the 6-picoline derivative of *cis,cis*-cyclohexane-1,3,5 tricarboxamide[25]. In this compound, which also crystallized in a trigonal space group (*R*3c), the cyclohexyl group was used to create disc-shaped molecules containing carboxamide groups at the periphery. A similar intra-column hydrogen bond network observed in H_3**3**$^{S\text{–mbz}}$ is present in Hamilton's system. However, the inter-column aryl interactions appear to be more extensive in H_3**3**$^{S\text{–mbz}}$ than in Hamilton's systems: this undoubtedly results from the increased order obtained by positioning chiral groups at the periphery of the tripodal arms in H_3**3**$^{S\text{–mbz}}$.

*Solid State Structure of [NEt$_4$]$_2$[Ni**3**$^{S-mbz}$(F)]*

The trianionic derivative [**3**$^{S-mbz}$]$^{3-}$, formed by deprotonating each amide group in H$_3$**3**$^{S-mbz}$, binds metal ions with tetradentate coordination[34,35]. The methylbenzyl groups appended to each amide nitrogen act as scaffolding for the generation of chiral cavities whose structures are affected by the binding of external ligands. The effects of placing a fluoride ion inside a chiral cavity were examined because of its relatively small radius and high electronegativity. Specifically, we wanted to investigate: i) if binding fluoride ions would order the methylbenzyl groups to form C_3-symmetric chiral complexes and ii) whether a non-centrosymmetic metal-containing lattice would form that had unusual structural features. [NEt$_4$]$_2$[Ni**3**$^{S-mbz}$(F)] crystallized as yellow block crystals in the non-centrosymmetic space group $P6_3$. The molecular structure of [Ni**3**$^{S-mbz}$(F)]$^{2-}$ is shown in Fig. (**17**) and reveals that the complex has a trigonal bipyramidal coordination geometry around the Ni(II) ion. The three amidate nitrogens of [**3**$^{S-mbz}$]$^{3-}$ are arranged in the trigonal plane with interplanar N$_{amid}$-Ni(1)-N$_{amid}$ angle of 116.54(7)°. The fluoro ligand is apically bonded to the Ni(II) center[26]. The bound fluoro ligand is positioned *trans* to nitrogen N(1) of [**3**$^{S-mbz}$]$^{3-}$ with the Ni ion located 0.39 Å above the trigonal plane toward the coordinated fluoride ion.

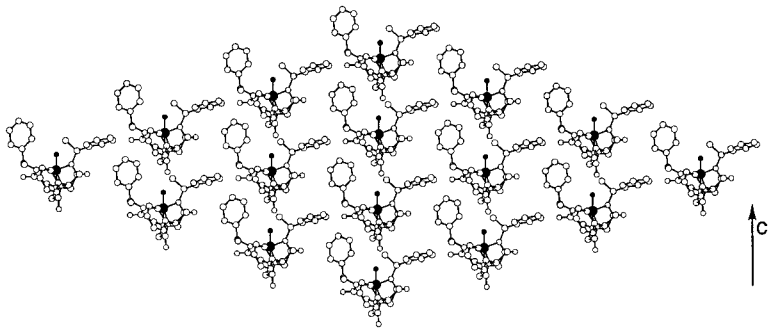

FIGURE 19 A portion of the crystal lattice for [Ni**3**$^{S-mbz}$(F)]$^{2-}$ showing the alignment of the Ni-F bonds. Hydrogens have been omitted for clarity

[Ni**3**$^{S-mbz}$(F)]$^{2-}$ possesses C_3 symmetry where the axis coincides with the F-Ni-N(1) vector. The appended methylbenzyl groups are thus sym-

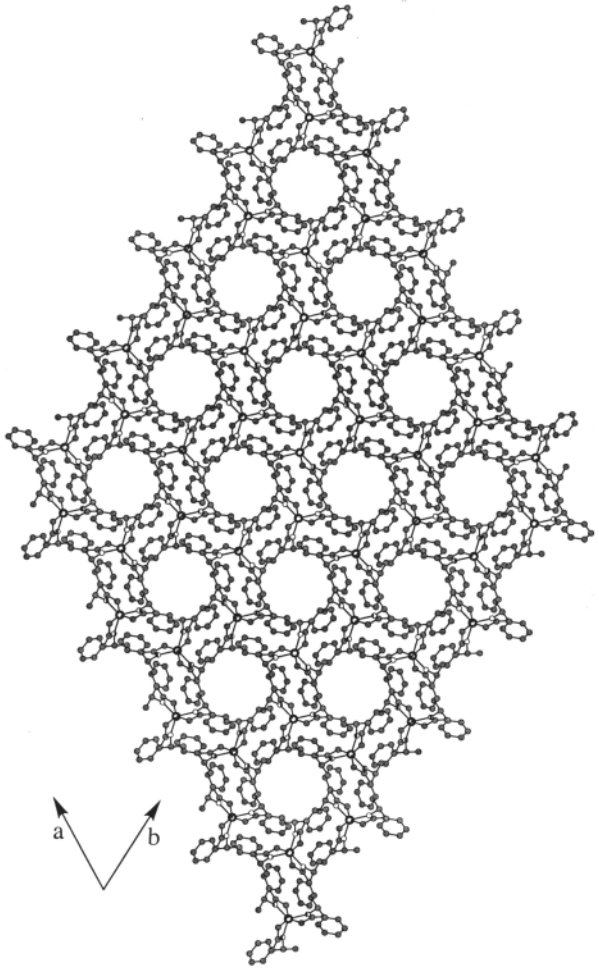

FIGURE 20 A portion of the crystal lattice for [Ni**3**$^{S-mbz}$(F)]$^{2-}$ illustrating the six-fold symmetric channels (viewed along the *a*,*b* plane). The Et_4N^+ ions and the hydrogens have been omitted for clarity

metrically disposed around the bonded fluoro ligand to form a chiral cavity of alternating aryl and methyl moieties. Each aryl ring in [Ni**3**$^{S-}$

$^{mbz}(F)]^{2-}$ is positioned such that the C(6) hydrogen is directed toward the coordinated fluoro ligand with a C(6)H···F distance of 2.251 Å. The methyl moieties of the appended groups also interact with the fluoro ligand where the C(4)H···F distance is 2.444 Å. Both of these distances are within the range reported for other systems which have CH···F interactions[27,28]. These CH···F interactions are of sufficient strength to direct, in part, the orientation of the methylbenzyl groups in the chiral cavity. Support for this suggestion comes from comparing the cavity structure in [Ni**3**$^{S-mbz}(F)]^{2-}$ to those found in the Zn(II) and Fe-NO complexes of [**3**$^{S-mbz}]^{3-}$ [34]. In these latter systems, the major intra-cavity interactions are Ph···Me that arise from interactions between adjacent arms. This type of interaction produces a cavity structure that is significantly different from that observed in [Ni**3**$^{S-mbz}(F)]^{2-}$ where intra-cavity Ph···Me interactions are absent.

Figs. (**18**) and (**19**) show the crystal lattice packing for $[NEt_4]_2$[Ni**3**$^{S-mbz}(F)]$. For this salt, the packing pattern in the *a*,*b* plane is similar to that found for H_3**3**$^{S-mbz}$: each anion is surrounded by six neighboring anions within the *a*,*b* plane where intermolecular edge-to-face aryl interactions are the dominant packing forces. The aryl groups of each tripodal arm are involved in two edge-to-face aryl interactions at a centroid-to-centroid distance of 5.622 Å. Layers of [Ni**3**$^{S-mbz}(F)]^{2-}$ anions are thus observed in the *a*,*b* plane with each anionic layer being separated by a layer of tetraethylammoniun cations (Fig. (**18b**)). Unfortunately, the ethyl groups of each cation are severely disordered and only the positions of the nitrogen atoms could be determined. Nevertheless, two potentially useful structural features can be obtained from the relative positioning of the anions and cations in the crystal lattice. All the Ni-F bonds in the [Ni**3**$^{S-mbz}(F)]^{2-}$ anions are oriented in the same direction, coincident with the crystallographic *c*-axis (Fig. **19**). This alignment of Ni-F bonds, which should have large dipoles, may lead this crystalline salt to have a large net dipole moment which is a prerequisite for important physical properties, such as nonlinear optical activity. Secondly, as illustrated in Fig. (**20**), six-fold symmetric channels are dispersed throughout the lattice that are walled by the chiral tripodal arms of the [Ni**3**$^{S-mbz}(F)]^{2-}$ anions. The channels in this lattice have diameters of ~11.5 Å and are filled with tetraethylammonium cations. The role of the cations in the channel formation is not presently known because the disorder in the ethyl groups has hindered any detailed structural analysis.

SUMMARY

Our work has shown that a diverse group of lattice architectures can be obtained using simple molecular templates as building blocks. C_2-symmetric derivatives of the template 2,6-bis(carbamoyl)pyridine, form compounds with helical or planar molecular structures. These molecular species assemble into open-framework, columnar, and helical lattice motifs, many of which are members of non-centrosymmetric space groups. The varied nature of these lattice types is a direct result of using weak metal-ligand interactions to control molecular structure. The self-complementary C_3-symmetric, tripodal compound $H_3\mathbf{3}^{S\text{–mbz}}$ also forms chiral crystals, as does a metallated derivative containing a Ni(II)-F moiety. The assembly processes in both symmetry types are driven by the clustering of weak electrostatic interactions such as hydrogen bonding and aryl-aryl interactions.

These results show the potential of these designs in forming new crystalline species. However, there is still much to learn about the growth of these complex lattice architectures. It is evident for our results that the precise control of intermolecular interactions is need to generate new crystals lattices. The control of these interactions from the molecular level will result ultimately in the ability to tune supramolecular structures to produce specific physical properties [29,30].

Acknowledgements

The author thanks his coworkers Drs. T. Kawamoto, B. Hammes and Q. Yu, for all their efforts. All the X-ray diffraction experiments described in this review was done in collaboration with Professor Arnie Rheingold (University of Delaware) and Dr. Victor Young, Jr. (University of Minnesota). It has been a pleasure to work with such excellent scientists. We thank the NIH (GM50781) and NSF EPSCoR Program (OSR-9255223) for financial support of this work.

References

[1] General references:
(a) Desiraju, G. D. *Crystal Engineering: The Design of Organic Solids*; Elsevier: New York, **1989**.
(b) Lehn, J.-M. *Angew. Chem., Int. Ed. Engl*. **1990**, *29*, 1304;
(c) *Transition Metals in Supramolecular Chemistry*, Fabbrizzi, L.; Poggi, A., Eds.; Kluwer Academic: Dordrecht, **1994**.

(d) Lehn, J.-M. *Supramolecular Chemistry* VCH: Weinheim, **1995**.
(e) *J. Coord. Chem*.; Borovik, A. S. and Aakeröy, C., Eds.; Elsevier Science B. V.: Amsterdam, **1999**, vol 183.

[2] Selected examples:
(a) Müller, A.; Reuter, H.; Dillinger, S.; *Angew. Chem., Int. Ed. Engl*. **1995**, *34*, 2328.
(b) Eichen, Y.; Lehn, J.-M.; Scherl, M.; Haarer, D.; Fischer, J.; DeCian, A.; Corval, A.; Trommsdorff, H. P. *Angew. Chem., Int. Ed. Engl*. **1995**, *34*, 2530.
(c) Frey, W.; Schief, W. R., Jr.; Pack, D. W.; Chen, C.-T.; Chilkoti, A.; Stayton, P.; Vogel, V.; Arnold, F. *Proc. Natl. Acad. Sci. USA* **1996**, *93*, 4937.
(d) Medina, J. C.; Gay, I.; Chen, Z.; Eschegoyen, L.; Gokel, G. W. *J. Am. Chem. Soc*. **1991**, *113*, 365.
(e) Saalfrank, R. W.; Stark, A.; Bremer, M.; Hummel, H.-U. *Angew. Chem., Int. Ed. Engl*. **1990**, *29*, 311.
(f) Copp, S. B.; Subramanian, S.; Zaworotko, M. *J. Chem. Soc., Chem. Comm*. **1993**, 1078.

[3] (a) Simard, M.; Su, D.; Wuest, J.D. *J*. D. *J. Am. Chem. Soc*. **1991**, *113*, 4696.
(b) Wang, X.; Simard, M.; Wuest, J.D. *J*. D. *J. Am. Chem. Soc*. **1994**, *116*, 12119.

[4] Selected examples:
(a) Aakeröy, C.B.; Nieuwenhuyzen, M. *J. Am. Chem. Soc*. **1994**, *116*, 10983.
(b) Aakeröy, C.B.; Nieuwenhuyzen, M. *J. Am. Chem. Soc* **1996**, *118*, 10134.
(c) Hanessian, S.; Gomtsyan, A.; Simard, M.; Roelens, S. *J. Am. Chem. Soc* **1994**, *116*, 4495.
(d) Zerkowski, J. A.; Mathias, J. P.; Whitesides, G. M. *J. Am. Chem. Soc* **1994**, *116*, 4305.
(e) Kolotuchin, S. V.; Zimmerman, S. C. *J. Am. Chem. Soc* **1998**, *120*, 9092.

[5] (a) Fujita, M.; Kwon, Y. J.; Washizu, S.; Ogura, K. *J. Am. Chem. Soc*. **1994**, *116*, 1151.
(b) Gardner, G. B.; Venkataraman, D.; Moore, J. S.; Lee, S. *Nature*, **1995**, *374*, 792.
(c) Yaghi, O. M.; Li, G.; Li, H. *Nature*, **1995**, *374*, 792.
(d) Robson, R. In *Comprehensive Supramolecular Chemistry*; Atwood, J.; Davies, J. E. D.; MacNicol, D. D.; Vögtle, F., Eds.; Elsevier Science: Oxford, England, 1996; p. 773.
(e) Hirsch, K. A.; Wilson, S. R.; Moore, J. S. *Inorg. Chem*. **1997**, *36*, 2960.

[6] (a) Lehn, J.-M.; Rigault, A.; Siegel, J.; Harrowfield, J.; Chevier, B.; Moras, D. *Proc. Natl. Acad. Sci., USA* **1987**, *84*, 2565.
(b) Dietrich-Buchecker, C. O.; Sauvage, J.-M. *Angew. Chem., Int. Ed. Engl*. **1989**, *28*, 189.
(c) Constable, E. D.; Elder, S. M.; Healy, J.; Ward, M. D.; Tocher, D. A. *J. Am. Chem. Soc*. **1990**, *112*, 4590.
(d) Piguet, C.; Bernardinelli, G.; Bocquet, B.; Quattropani, A.; Williams, A. F. *J. Am. Chem. Soc*. **1992**, *114*, 7440.

[7] (a) Kawamoto, T.; Prakash, O.; Ostrander, R.; Rheingold, A. L.; Borovik, A. S. *Inorg. Chem*. **1995**, *34*, 4294.
(b) Kawamoto, T.; Hammes, B. S.; Haggerty, B.; Yap, G. P. A.; Rheingold, A. L.; Borovik, A. S. *J. Am. Chem. Soc*. **1996**, *118*, 285.
(c) Yu, Q.; Baroni, T. E.; Liable-Sands, L. M.; Rheingold, A. L.; Borovik, A. S. *Tetrahedron Lett*. **1998**, *38*, 6831.
(d) Kawamoto, T.; Hammes, B.S.; Ostrander, R.; Rheingold, A.L.; Borovik, A.S. *Inorg*. *Chem*. **1998**, *37*, 3424.
(e) Hammes, B. S.; Ramos-Maldonado,D.; Yap, G. P. A.; Rheingold, A. L.; Young, V. G., Jr.; Borovik, A. S. *Coord. Chem. Rev*. **1998**, *174*, 241.

(f) Yu, Y., Baroni, T. E.; Liable-Sands, L. M.; Yap, G. P. A.; Rheingold, A L.; Borovik, A. S. *Chem. Commun*. **1999**, *6*, 553.
[8] General references for hydrogen bonding interactions:
(a) Etter, M.C. *Acc. Chem. Res*. **1990**, *23*, 120.
(b) Aakeröy, C.; K.R. Seddon *Chem. Soc. Rev*. **1993**, *22*, 397.
(c) Aakeröy, C.B.; Nieuwenhuyzen, M. *J. Mol. Struct*. **1996**, *374*, 223.
[9] General references for aryl interactions:
(a) Burley S. K.; and Petsko, G. A. *J. Am. Chem. Soc*. **1986**, *108*, 7995.
(b) Hunter, C. A.; Sanders, J. K. M. *J*. K. M. J. *Am. Chem. Soc*. **1990**, *112*, 5525.
(c) Hunter, C. A. *Chem. Soc. Rev*. **1994**, 101, and references therein.
(d) Hobza, P.; Selzle, H. L.; Schlag, E. W. *J. Am. Chem. Soc*. **1994**, *116*, 3500.
[10] (a) Hirshmann, R. *Angew. Chem., Int. Ed. Engl*. **1991**, *30*, 1278.
(b) Kahn, M. *Synlett* **1993**, 821.
(c) Ernest, I.; Kalvoda, J.; Rihs, G.; Mutter, M. *Tetrahedron Lett*. **1990**, *31*, 4011.
(d) Feigel, M. *J. Am. Chem. Soc*. **1986**, *108*, 181.
(e) Kahn, M.; Bertenshaw, C. M. *Tetrahedron Lett*. **1989**, *30*, 2317.
(f) Kahn, M.; Wilke, S.; Chen, B.; Fujita, K. *J. Am. Chem. Soc*. **1988**, *110*, 1638.
(g) Kemp, D. S.; Bowen, B. R. *Tetrahedron Lett*. **1988**, *29*, 5077.
(h) Kemp, D. S.; Stites, W. E. *Tetrahedron Lett*. **1988**, *29*, 5057.
(i) Kelly, J. W.; Schneider, J. P. *Chem. Rev*. **1995**, *95*, 2169–2187.
(j) Mutter, M.; Tuchscherer, G.; Servis, C.; Corradin, G.; Blum, U.; Rivier, J. *Protein Science* **1992**, *1*, 1377.
(k) Diaz, H.; Graciani, N. *J. Am. Chem. Soc*. **1994**, *116*, 3988.
(1) Kelly, J. W.; Nesloney, C. L. *J. Am. Chem. Soc*. **1996**, *118*, 5836.
(m) Gellman, S. H. *Acc. Chem. Res*. **1998**, *31*, 173.
(n) Nowick, J. S. *Acc. Chem. Res*. **1999**, *32*, 287.
[11] Notable exception: Schneider, J. P.; Kelly, J. W. *J. Am. Chem. Soc*. **1995**, *117*, 2533.
[12] Alber, T. *Prediction of Protein Structure and the Principles of Protein Conformation*; Fasman, G. D.; Ed.; Plenum Press: New York, 1989.
[13] Sorrell, T. N. *Interpreting Spectra of Organic Molecules*; University Science Books: Mill Valley, CA, **1988**, p 24.
[14] Examples of metal complexes with mulitdentate ligands that form helical structures:
(a) Lindoy, L. F.; Busch, D. H. *J. Chem.Soc., Chem. Soc., Chem. Comm*. **1972**, 683.
(b) Wester, D.; Palenik, G.J. *J*. J. *Chem.Soc., Chem. Comm*. **1975**, 74.
(c) Lehn, J.-M.; Rigault, A. *Angew. Chem., Int. Ed. Engl*. **1988**, *27*, 1095.
(d) Williams, A. F.; Piquet, C.; Bernardinelli, G. *Angew. Chem*., *Int. Ed. Engl*. **1991**, *30*, 1490.
[15] (a) Alyea, E. C.; Ferguson, G.; Restivo, R. J. *Inorg. Chem*. **1975**, *14*, 2491.
(b) Wester, D.; Palenik, G. J. *J. Am. Chem. Soc*. **1975**, *96*, 7565.
(c) Alcock, N. W.; Moore, P.; Reader, C. J.; Roe, S. M. *J. Chem. Soc., Dalton Trans*. **1988**, 2959.
(d) Krüger, H.-J.; Holm, R. H. *J. Am. Chem. Soc*. **1990**, *112*, 2955.
(e) Grove, D. M.; van Koten, G.; Ubbels, H. J. C.; Zoet, R.; Spek, A. L. *Organometallics*, **1984**, *3*, 1003.
[16] *CRC Handbook of Chemistry and Physics*; 53rd Edition; Weast, R. C., Ed.; CRC Press: Boca Raton, FL, **1972**; p. F180.
[17] Examples of π-stacking interactions in supramolecular chemistry see:
(a) Desiraju, G. D. *Crystal Engineering: The Design of Organic Solids*; Elsevier: New York, 1989.
(b) Hunter, C. A. *Chem. Soc. Rev*. **1994**, 101, and references therein.
[18] (a) Hamuro, Y.; Geib, S. J.; Hamilton, A. D. *Angew. Chem. Int. Ed. Engl*. **1994**, *33*, 446.

(b) Goodman, M. S.; Hamilton, A. D.; Weiss, J. *J. Am. Chem. Soc*. **1995**, *117*, 8447.
(c) Hamuro, Y.; Geib, S. J.; Hamilton, A. J. *J. Am. Chem. Soc*. **1997**, *119*, 587.
[19] Pirkle, W. H.; Hoekstra, M. S. *J. Am. Chem. Soc*. **1976**, *98*, 1832.
[20] Cahn, R. S.; Ingold, C; Prelog, V. *Angew. Chem. Int., Ed. Engl*. **1966**, *5*, 385.
[21] Examples of other systems that use edge-on aromatic interactions:
(a) Protein secondary and tertiary structure: Burley, S. K.; Petsko, G. A. *Science* (*Washington, D. C.*) **1985**, *229*, 23.
(b) Crystal lattices of aromatic molecules: Desiraju, G. R.; Gavezzotti, A. *J. Chem. Soc., Chem. Commun*. **1989**, 621 and references therein.
(c) To effect stereoselectivity in metal complexes: Karpishin, T. B.; Stack, T. D. P.; Raymond, K. *N. J. Am. Chem. Soc*. **1993** *115*, 6115.
(d) In molecular recognition: Muehldorf, A. V.; Van Engen, D.; Warner, J. C.; Hamilton, A. D. *J. Am. Chem. Soc*. **1988**, *110*, 6561; Hunter, C. A. *J. Chem. Soc., Chem. Commun*. **1991**, 749.
[22] Hammes, B. S.; Maldonado-Ramos, D.; Yap, G. P. A.; Liable-Sands, L.; Rheingold, A. L.; Borovik, A. S. *Inorg. Chem*. **1997**, *36*, 3210.
[23] (a) M. Ray, G. P. A. Yap, A. L. Rheingold, A. S. Borovik, *J. Chem. Soc. Chem, Commun*. **1995**, 1777.
(b) M. Ray, A. P. Golombek, M. P. Hendrich, V. G. Young, A. S. Borovik, *J. Am. Chem. Soc*. **1996**, *118*, 6084.
(c) Shirin, Z.; Young, V. G.; Borovik, A. S. *Chem. Commun*. **1997**, *4*, 1840.
(d) Ray, M; Hammes, B. S.; Yap, G. P. A.; Rheingold, Liable-Sands, L.; Borovik, A. S *Inorg. Chem*. **1998**, *37*, 1527.
(e) Ray, M; Golombek, A.; Hendrich, M. P.; Yap, G. P. A.; Liable-Sands, L.; Rheingold, A. L.; Borovik, A. S. *Inorg. Chem*. **1999**, *38*, 3110.
[24] For the use of self-complementary molecules in assembly processes see: Wyler, R.; de Mendoza, J.; Rebek, J., Jr. *Angew. Chem. Int. Ed. Engl*., **1993**, *32*, 1699.
[25] Erkang, F.; Yang, J.; Geib, J. S.; Stoner, T. C.; Hopkins, M. D.; Hamilton, A. D. *J. Chem. Soc., Chem. Commun*. **1995**, 1251.
[26] (a) Emsley, J.; Arif, M. *J. Chem. Soc., Dalton Trans*. **1989**, 1273.
(b) Halasyamani, P.; Willis, M. J.; Stern, C. L.; Poeppelmeier, K. R. *Inorg. Chim. Acta*, **1995**, *240*, 109.
(c) Toriumi, K.; Ito, T. *Acta Cryst*., **1981**, *B37*, 240.
[27] Murray-Rust, P.; Stallings, W. C.; Monti, C. T.; Preston, R. K.; Glusker, J. P. *J. Am. Chem. Soc*. **1983**, *105*, 3207.
[28] Desiraju, G.R. *Angew. Chem. Int. Ed. Engl*. **1995**, *34* 2311.
[29] Brown, M. E.; Hollingsworth, M. D *Nature (London)*, **1995**, *376*, 323.
[30] For an example of using 2,6-bis(carbamoyl)pyridine units in dendrimers, see: Recker, J.; Tomcik, D. J.; Parquette, J. R. *J. Am. Chem. Soc*. **2000**; *122*, 10298.